



Ccp1 modulates epigenetic stability at centromeres and affects heterochromatin distribution in *Schizosaccharomyces pombe*

Received for publication, May 8, 2018, and in revised form, June 2, 2018. Published, Papers in Press, June 13, 2018, DOI 10.1074/jbc.RA118.003873

Min Lu and Xiangwei He¹

From the Life Sciences Institute and Innovation Center for Cell Signaling Network, Zhejiang University, Hangzhou, Zhejiang 310058, China

Edited by Xiao-Fan Wang

Distinct chromatin organization features, such as centromeres and heterochromatin domains, are inherited epigenetically. However, the mechanisms that modulate the accuracy of epigenetic inheritance, especially at the individual nucleosome level, are not well-understood. Here, using ChIP and next-generation sequencing (ChIP-Seq), we characterized Ccp1, a homolog of the histone chaperone Vps75 in budding yeast that functions in centromere chromatin duplication and heterochromatin maintenance in fission yeast (*Schizosaccharomyces pombe*). We show that Ccp1 is enriched at the central core regions of the centromeres. Of note, among all histone chaperones characterized, deletion of the *ccp1* gene uniquely reduced the rate of epigenetic switching, manifested as position effect variegation within the centromeric core region (CEN-PEV). In contrast, gene deletion of other histone chaperones either elevated the PEV switching rates or did not affect centromeric PEV. Ccp1 and the kinetochore components Mis6 and Sim4 were mutually dependent for centromere or kinetochore association at the proper levels. Moreover, Ccp1 influenced heterochromatin distribution at multiple loci in the genome, including the subtelomeric and the pericentromeric regions. We also found that Gar2, a protein predominantly enriched in the nucleolus, functions similarly to Ccp1 in modulating the epigenetic stability of centromeric regions, although its mechanism remained unclear. Together, our results identify Ccp1 as an important player in modulating epigenetic stability and maintaining proper organization of multiple chromatin domains throughout the fission yeast genome.

Nucleosomes, the basic structural units of chromatin, are each composed of two copies of histone H3, H4, H2A, and H2B, respectively, with a 147-bp DNA fragment wrapping around (1). Distinct nucleosomal organization patterns along the chromatin profoundly affect the functional output of the genome

This work was supported by National 973 Plan for Basic Research Grant 2015CB910602 (to X. H.) and National Natural Science Foundation of China (NSFC) Grant 31628012 (to X. H.). The authors declare that they have no conflicts of interest with the contents of this article.

This article contains Tables S1–S3 and Figs. S1–S6.

ChIP-Seq data and the details of data analysis procedures have been submitted to the NCBI Gene Expression Omnibus (GEO) under accession number GSE95047.

¹ To whom correspondence should be addressed. Tel.: 86-751-88206639; E-mail: xhe@zju.edu.cn.

and must be preserved during cell proliferation to maintain specific transcription program and, thereby, the distinct cell identity. The chromatin is duplicated along with DNA replication via a process called replication-coupled nucleosome assembly (2, 3). To duplicate the chromatin structure accurately, it is essential that the recycled old histones (which may carry the epigenetic information) should be reincorporated into their original sites on one of the duplicated DNA strands. Furthermore, on the other daughter DNA strand, the same nucleosome organization pattern needs to be established *de novo*, using newly synthesized histones (4–6).

In the past decades, much has been learned about the biological processes that influence genetic stability, including DNA replication precision, DNA damage and repair, and cell death with severe DNA damage. In comparison, little is known about how epigenetic stability is achieved, which must be influenced by the precision of chromatin duplication and almost certainly other processes that implicate chromatin, such as transcription and DNA damage repair.

Not all chromosomal features are necessarily inherited epigenetically, with some better demonstrated than others. One well-established example is the centromere, a site of the chromosome on which the kinetochore assembles. The kinetochore is a large multiprotein apparatus that links the chromosome to the spindle microtubules and provides the physical force driving chromosome segregation in mitosis and meiosis (7–9). The location of the centromere is epigenetically determined by CENP-A (a centromere-specific histone H3 variant) containing nucleosomes in eukaryotes. In general, the DNA sequence underlying centromeric chromatin is neither necessary nor sufficient for centromere assembly, except for the budding yeast, whose centromere is determined by specific DNA sequence and is composed of only one Cse4 (CENP-A homolog) containing nucleosome (10–12). Most eukaryotic organisms, including the fission yeast, have a large and complex centromere on each chromosome, containing dozens to hundreds of CENP-A nucleosomes. Although CENP-A nucleosomes are exclusively localized to centromeres, canonical H3 nucleosomes also exist within centromeres, interspersing with CENP-A nucleosomes (13–15).

Another well-established epigenetic feature is the heterochromatin (16). Studies have shown that the heterochromatin formation pathways are highly conserved (17–19). In the fission yeast *Schizosaccharomyces pombe*, the pericentromeric and subtelomeric regions and the silent mating-type locus are

coated with heterochromatin (20–22). At the junctions of the pericentromeric and the central core regions of the centromere, the boundaries between the two domains are well-defined by the underlying tRNA genes (23). No heterochromatin is detected within the central core regions.

We are interested in exploring what may influence the accuracy of chromatin duplication, using fission yeast as the experimental system. Any inheritable changes occurred during the history of colony formation may be preserved and reflected in the heterogeneity and complexity of the cell population within the colony and can be assessed qualitatively and quantitatively (24). We notice that epigenetic inheritance of a specific chromatin feature may be readily manifested by a phenomenon called position effect variegation (PEV),² in which the transcription state of a gene, due to its specific locus within the genome, varies between a repressed mode and an expressed mode. PEV was first reported in the 1930s in specific *Drosophila* mutant strains where the *white* gene expression status was variable upon translocation to a site nearby heterochromatin (25), reflecting the dynamic changes of heterochromatin spreading onto or shrinking from the *white* gene. PEV was later observed broadly in other organisms and is associated with various underlying chromatin features. In fission yeast, PEV was observed with a reporter gene (e.g. *ade6* or *ura4*) inserted within the centromeric core region (referred to as CEN-PEV in this work) (26). Subsequent studies, including those from our laboratory, have demonstrated that in CEN-PEV, Cnp1 (CENP-A homolog in fission yeast) nucleosome occupancy on the reporter gene correlates with its transcriptional silencing (15, 27, 28).

Using an experimental procedure, the pedigree analysis, to track the ON and OFF states of the *CEN::ade6* reporter through mitotic cell generations at the individual cell level, we have shown that the transcription states of *CEN::ade6* are inheritable through cell generations. Switches between the two states are also detected at constant rates (15). CEN-PEV vividly reflects the epigenetic inheritance and the dynamic switching of centromeric chromatin states. Given the correlation between Cnp1 occupancy and the silencing of the reporter genes, these interchangeable chromatin states likely correlate with changes in Cnp1 nucleosome positioning within the centromeric core.

PEV also occurs elsewhere in the fission yeast genome, such as the subtelomeric region or next to a heterochromatin-initiating DNA element (*cenH*). There, instead of Cnp1 occupancy, gene silencing is due to heterochromatin (H3K9me2) spreading onto or shrinking from the reporter (29). In sum, despite the different biochemical nature of the associated chromatin features, PEV may serve as a convenient indicator of epigenetic inheritance stability of local chromatin structures through mitotic cell generations.

Here we describe characterizing new roles of Ccp1 in fission yeast, as an important modulator for the epigenetic stability of PEVs associated with Cnp1 or heterochromatin modification (H3K9me2), centromere function, and proper heterochromatin

distributions elsewhere in the epigenome. Also, we have found that Gar2, a nucleolar protein, functionally cooperates with Ccp1 in maintaining proper heterochromatin distribution at pericentromeric regions as well as in modulating centromeric epigenetic stability.

Results

Deletion of *ccp1* causes reduction in the rates of PEV epigenetic switching at different loci

To elucidate the mechanism that modulates the nucleosomal epigenetic stability in fission yeast, we performed a genetic survey in an annotated gene deletion library (30). An established CEN-PEV system was used as the readout for the genetic screen in which a reporter gene, *ade6*, was inserted at the central core of *CEN2*. Previous studies indicated that the occupancy of Cnp1 on *ade6* correlates with transcriptional silencing (15, 27, 28, 31). We reason that, using centromeric PEV of *ade6* inserted in *cnt2* (designated as *cnt2::ade6* thereafter in this work) as the readout, switching between the ON and OFF states of *ade6* reflects the changes of Cnp1 occupancy on the *ade6* reporter gene through mitotic cell generations. The frequencies of such switches are visually illustrated by the intensities of color-sectoring strips of individual colonies, as the red and white colors are correspondent to *ade6* OFF and ON, respectively, in medium with low adenine supply. In an ongoing screening of the Bioneer V.1 *pombe* deletion library, we have identified specific genes whose deletion led to quantitative changes in *cnt2::ade6* expression pattern switching within single colonies. In selected isolates, we quantified the changes in switching frequencies by an established pedigree analysis assay (15) (see Fig. 1C). In this study, we focus on one gene, SPBC36B7.08c (systematic ID), named as *ccp1*, which encodes a protein homologous to a histone chaperone, Vps75, in the budding yeast.

Single colonies of *ccp1Δ* originated from *ade6* silencing cells are predominantly red and consistently contain fewer white sectors than those of WT, demonstrating that Cnp1 occupancy on *ade6* switches less frequently in the mutant (Fig. 1A). To test whether Ccp1 also affects the epigenetic stability elsewhere on chromatin mediated by canonical H3 nucleosomes, we assessed the variability of PEV associated with heterochromatin. Specifically, a DNA segment, *cenH* (centromere-homologous repeat) element within the mating-type region, is sufficient to initiate the formation of heterochromatin at ectopic sites via an RNAi-dependent pathway (32). By inserting *cenH* at the *ura4* locus and placing *ade6* next to *cenH* (designated as *cenH::ade6* in this work thereafter), a typical PEV phenomenon is observed (Fig. 1B). Compared with WT, *ccp1Δ* colonies showed the reduced variability of *cenH::ade6* PEV, based on colony morphology of color sectoring density (Fig. 1B). Quantification by pedigree analysis confirmed that the switching rates of both *cnt2::ade6* (also see Fig. 7B in Ref. 15) and *cenH::ade6* were reduced in *ccp1Δ* compared with WT (Fig. 1C).

Ccp1 shows a high structural similarity to Vps75, suggesting that it may function as an authentic histone chaperone (33). In budding yeast, Vps75 was shown to form a complex with Rtt109 and to promote Rtt109's acetyltransferase activity on Lys-56 of histone H3 (34, 35). An Rtt109-independent role of Vps75 was

² The abbreviations used are: PEV, position effect variegation; CEN, centromeric core region; H3K9me2, histone H3 Lys-9 dimethylation; SPB, spindle pole body; TBZ, thiabendazole; DIC, differential interference contrast.

Nucleosomal epigenetic stability regulated by Ccp1

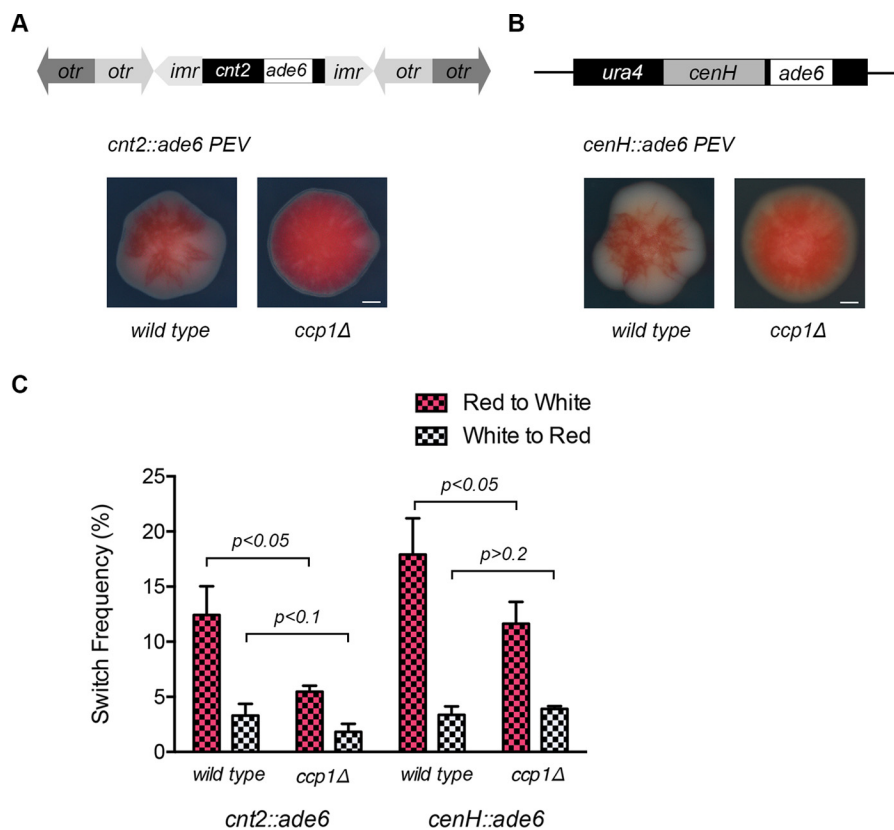


Figure 1. *ccp1Δ* reduces the rates of PEV epigenetic switching at both *cnt2::ade6* and *cenH::ade6*. A and B, schematics of the reporter gene *ade6* insertion sites at genome. Representative colonies that are mostly red (hence, derived from an *ade6*-silenced ancestor cell) are shown. Colony color sectoring morphology is compared between WT and *ccp1Δ*. Both *cnt2::ade6* PEV (A) and *cenH::ade6* PEV (B) of *ccp1Δ* showed fewer sectors than WT. Scale bar, 50 μ m. C, quantification of the red-to-white and white-to-red switching rates in *ccp1Δ* and WT (total cell divisions counted: $n > 600$). The S.D. (error bars) is calculated by randomly subgrouping cell pedigrees into three parts (each part contained about 200 cell division events). p values are calculated by t test.

also reported (36). To test whether the role that Ccp1 (Vps75 homolog) plays in nucleosomal epigenetic stability is linked with Rtt109, we examined the PEV phenotype of the *rtt109Δ* strain and found that *rtt109Δ* does not affect the variability of *cnt2::ade6* (consistent with our previous result (Fig. 7B in Ref. 15) or that of *cenH::ade6* (Fig. S1A). Hence, our data indicate that Ccp1 modulates the nucleosomal epigenetic stability in an Rtt109-independent manner.

Vps75 belongs to the NAP (nucleosome assembly protein) family and functions as a histone chaperone that binds with histone H3-H4 tetramer (37, 38). This prompted us to investigate whether other histone chaperones or chromatin remodeling factors play a role in modulating *cnt2::ade6* PEV and *cenH::ade6* PEV variability. To this end, we constructed deletion strains for a list of candidate genes, combining the deletions with the *cnt2::ade6* or *cenH::ade6* reporters by genetic crossing. PEV phenotypes were examined by visual inspection of the colony color-sectoring morphology. The results (summarized in Table 1 and Fig. S1B) suggest that whereas most candidate gene deletions either do not affect the epigenetic stability of the reporters at all or enhance the epigenetic switching in only *cnt2::ade6*, *ccp1Δ* uniquely causes reduction in nucleosomal epigenetic switching that is mediated by both Cnp1 (*cnt2::ade6*) and H3K9me2 (*cenH::ade6* marker inserted in *ura4* locus).

Table 1

A summary of the epigenetic stability characterization of selected chromatin modulator mutants using the *cnt2::ade6* and *cenH::ade6* PEV systems

Enhanced and Reduced, the epigenetic switching frequency higher and lower, respectively, than the WT; WT-like, WT level; White Colony, lack of *ade6* silencing.

<i>S. pombe</i> proteins	Homologues in <i>Homo sapiens</i>	<i>cnt2::ade6</i> PEV	<i>cenH::ade6</i> PEV
Pcf1	Chromatin assembly factor (CAF-1)	Enhanced	Reduced
Pcf2		WT-like	WT-like
Pcf3		WT-like	WT-like
Slm9	Histone cell cycle regulation defective homologue A (HIRA)	Enhanced	WT-like
Hip1		Enhanced	White Colony
Mug183	Regulator of Ty transposition (Rtt106)	WT-like	WT-like
Chz1	Chz1 (Histone H2A.Z-specific chaperone)	WT-like	WT-like
Nap1	Nucleosome assembly protein (NAP)	WT-like	WT-like
Nap2		Enhanced	WT-like
Ccp1	SET (nuclear proto-oncogene)	Reduced	Reduced
Rtt109	None	WT-like	WT-like
Nhp6	SSRP1 (Structure specific recognition protein 1)	WT-like	WT-like
SPAC27F1.06c	None	WT-like	WT-like
Brl2	Ring finger protein (RNF)	White Colony	White Colony

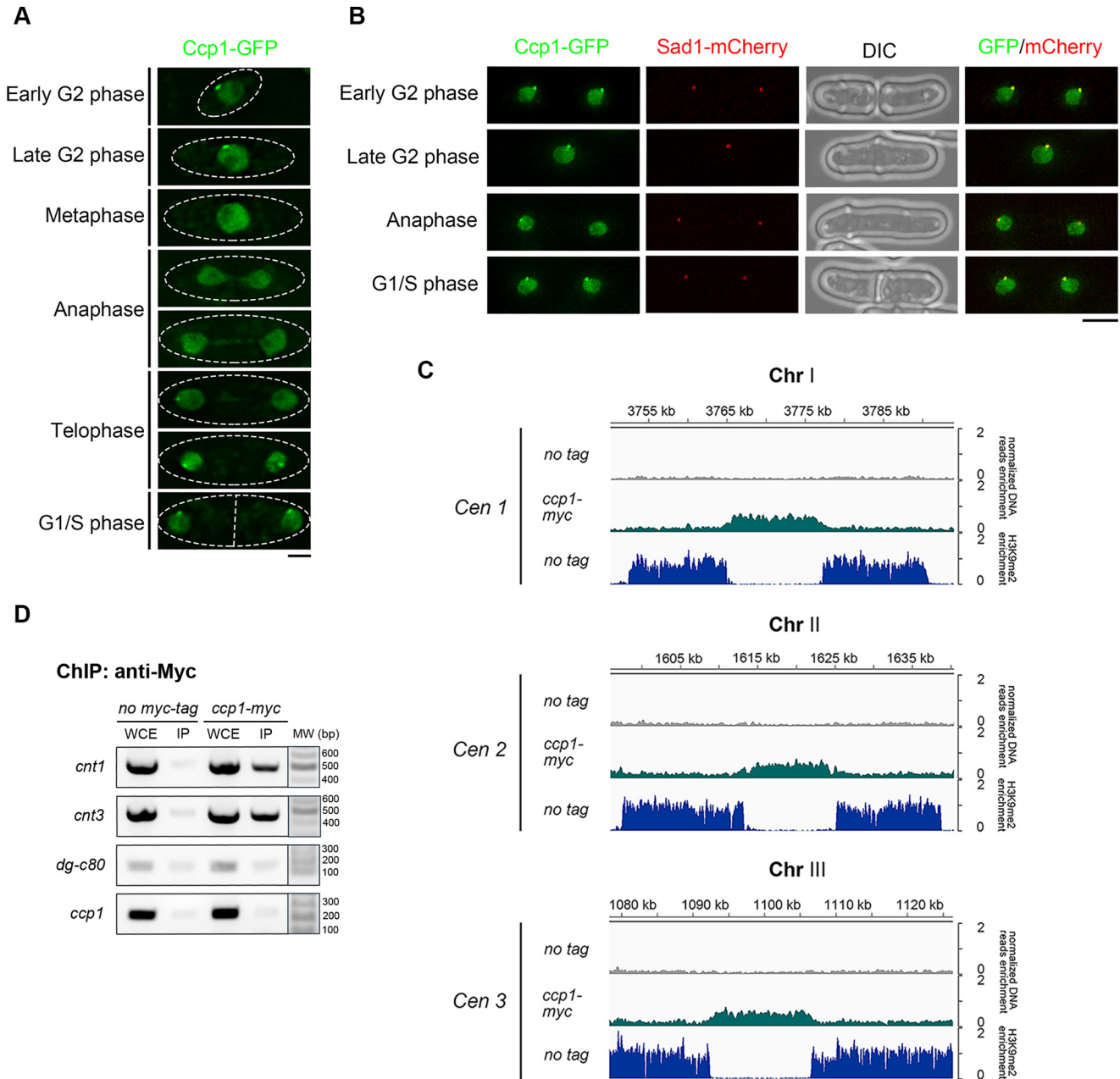


Figure 2. Ccp1 is enriched at centromeres and specifically binds to the central core regions. *A*, representative images of cells expressing Ccp1-GFP. Different cell cycle phases were shown: interphase (G₁-G₂ phase), metaphase, anaphase, and telophase. Scale bar, 2 μm. *B*, co-localization of Ccp1-GFP (green) and the SPB marker Sad1-mCherry (red). Cell outlines are shown in DIC images. Merged images (green and red) are displayed at the right. Scale bar, 5 μm. *C*, Myc ChIP-Seq of Ccp1-Myc (green), with no tag as the negative control (gray), showed the specific binding profile of Ccp1 at centromeres. All three *S. pombe* centromeres are shown. The pericentromeric heterochromatin H3K9me2 distribution in WT cells (blue) was displayed to distinguish inner and outer regions of centromeres (H3K9me2 only exists in outer repetitive regions). y axis, Myc ChIP-Seq reads normalized for DNA read enrichment. x axis, chromosomal position of the centromeres. *D*, anti-Myc ChIP-PCR analysis of a negative control (no tag) and a Ccp1-Myc. The primers corresponding to the central core of the centromeres (*cnt1*, *cnt3*), pericentromeric heterochromatin (*otr* region, *dg-c80*), and a euchromatin gene (SPBC36B7.08c, *ccp1*) are listed in Table S3. IP, immunoprecipitation.

Ccp1 binds to the central core regions of the centromeres

Vps75 has a classical nuclear localization signal and is located in the nucleus in budding yeast (39). To examine the intracellular localization of Ccp1 in *S. pombe*, we fused a GFP tag to the C terminus of *ccp1* at its endogenous locus. We observed that Ccp1-GFP expressed under its native promoter is distributed throughout the nucleus at all cell cycle stages. In addition, during interphase (G₁ to G₂ phase) but not in mitosis, Ccp1-GFP forms a distinct bright dot at the edge of the nucleus (Fig. 2A), a

similar cellular localization pattern was also observed by Dong *et al.* (33). In fission yeast cells, all three centromeres cluster adjacent to the spindle pole body (SPB) at the nuclear periphery in interphase. To test whether the specific dot of Ccp1-GFP represents its enrichment at the centromeres/kinetochores, we assessed possible co-localization of the Ccp1-GFP dot with the SPB and the centromere/kinetochore cluster. In strains carrying Ccp1-GFP and Sad1-mCherry (an SPB protein) or Ccp1-DsRed1 and Spc7-GFP (a kinetochore component), with all

Nucleosomal epigenetic stability regulated by Ccp1

tagged genes under their respective native promoters (Fig. 2B and Fig. S1C), we found that the Ccp1-GFP dot overlaps with the SPB or the kinetochore dot, suggesting that Ccp1 in interphase is enriched at the centromeres/kinetochores.

The centromeres of fission yeast consist of a central core region (*cnt* and part of *imr*) and the flanking repetitive (*otr* and part of *imr*) sequence. Cnp1-containing nucleosomes are exclusively localized to the central core regions, and the flanking repetitive sequence is covered by constitutive heterochromatin. To determine the association sites of Ccp1 with the centromeres and to characterize the global distribution pattern of Ccp1 throughout the genome, ChIP plus next-generation sequencing (ChIP-Seq) were performed for Myc-tagged Ccp1 (C-terminal fusion protein). The result revealed that Ccp1 exclusively associates with the central core region of each centromere, which corroborates and expands the subcellular fluorescent observation results (Fig. 2C) (33). ChIP-PCR verified the specific enrichment of Ccp1 at the central core regions of the centromeres (Fig. 2D). Although *ccp1Δ* exhibited reduced sectoring in the *cenH::ade6* PEV system, we did not detect Ccp1 enrichment at any loci other than the centromeric cores reproducibly by ChIP-Seq. It is possible that Ccp1 may be associated transiently and/or weakly with specific loci other than centromeres, or it may be associated with chromatin broadly but nonspecifically throughout the genome that cannot be detected reliably with the current ChIP-Seq method, or Ccp1 has an indirect effect on these noncentromeric regions. In sum, these data showed that Ccp1 binds prominently with centromeres and thus may affect the epigenetic dynamics of the underlying centromeric nucleosomes via a direct interaction.

ccp1Δ affects the mitotic function of centromeres but does not alter the total level of Cnp1 incorporation

Based on the observation that Ccp1 specifically binds to centromeres, we hypothesized that *ccp1Δ* might affect the total level of Cnp1 occupancy at the centromeres. Dong *et al.* (33) showed about 12% of cells having multiple foci or diffuse signals in *ccp1Δ* carrying an ectopic Cnp1-GFP (also see “Discussion”). To test this with the endogenous level of Cnp1 expression, we microscopically examined WT and *ccp1Δ* carrying endogenous *cnp1-gfp*. To minimize experimental variations, we quantified the fluorescent intensity of the Cnp1-GFP dot in late G₂ phase cells (single-nucleus cells with length >10 μm). Cnp1-GFP forms a single dot, and its fluorescence intensity does not change significantly with *ccp1* deletion, suggesting that Ccp1 does not affect the total amount of Cnp1 incorporated into the centromeres (Fig. 3, A and B).

The systematic survey of genetic interaction (epistasis mapping, E-MAP) in fission yeast provides important clues of functional networks of diverse biological processes (40). Analysis of epistasis mapping profiles showed that Ccp1 is functionally associated with the DASH complex. DASH complex mediates the interaction between the kinetochore and the spindle microtubules and is important for accurate chromosome segregation (41, 42). To verify and expand the results of E-MAP survey, we constructed double deletions of *ccp1* and multiple single components of DASH complex (*ccp1Δask1Δ* and *ccp1Δdad2Δ*) and

found that the double mutations displayed increased sensitivity to the microtubule-destabilizing drug thiabendazole (TBZ) (Fig. 3C). This is consistent with the speculation that Ccp1 plays a role in proper function of centromeres/kinetochores. In addition to the DASH complex, we also examined the genetic interaction between Ccp1 and other kinetochore components. *ccp1Δmis6-302* cells exhibited hypersensitivity to the microtubule-destabilizing drug TBZ (Fig. 3D) and severe growth defects when temperature exceeded 25 °C.

Ccp1 and the inner kinetochore protein Mis6 are mutually dependent for proper localization

To explore how Ccp1 is specifically enriched at centromeres/kinetochores, we tested inactivation or deletion mutations of several candidate genes, mainly including kinetochore protein-encoding genes. Most of these mutants, including *mis12-537*, *mis15-68*, and *fta6Δ*, do not affect Ccp1-GFP centromeric dot formation (Fig. 4A and Fig. S2A). In contrast, inactivation of Mis6 profoundly affects Ccp1 enrichment on centromeres. At the permissive temperature (26 °C), *mis6-302* mutant cells already had diminished fluorescent intensity in Ccp1-GFP dots. At the nonpermissive temperature (36 °C), Ccp1-GFP centromeric localization is completely abolished by microscopic examination (Fig. 4A). Thus, Ccp1 enrichment at the centromeres is specifically dependent on Mis6.

We next assessed whether Ccp1 has an impact on kinetochore assembly. Mis6–Mal2–Sim4 complex forms part of the inner centromeres, whereas Mis12, Ndc80, and Spc7 are outer kinetochore components. In *ccp1Δ* cells, there is 40–50% reduction in average Mis6-GFP and Sim4-GFP dot fluorescent intensity (Fig. 4, B and C), whereas Mis12-GFP (Fig. 4, B and C), Mis15-GFP, Ndc80-GFP, and Spc7-GFP maintain the same levels at centromeres compared with WT cells (Fig. S2, B and C). These results suggest that Ccp1 is required for the normal level incorporation of the Mis6-Sim4 branch of inner kinetochore components.

Nucleolar protein Gar2 genetically interacts with Ccp1 to regulate centromeric nucleosomal epigenetic stability

To gain further insight into the mechanism by which Ccp1 regulates the nucleosomal epigenetic stability, we affinity-purified endogenously expressed Ccp1-TAP and its associated proteins from the whole-cell extract. Mass spectrometry analyses revealed that histones were co-purified with Ccp1-TAP, consistent with its postulated role as a histone chaperone (Table S1). In addition to histones, one possible chromatin-associated protein, Gar2, was consistently co-purified with Ccp1 in both biological repeats, but not in the negative controls. Gar2 was implicated as a nucleolus protein by homology and a genome-wide protein localization survey (43–47). To test whether it is functionally related with Ccp1, we assessed the nucleosomal epigenetic switching rates in *gar2Δ* cells. Using the *cnt2::ade6* PEV system, *gar2Δ* displayed reduced epigenetic switching similar to *ccp1Δ* (Fig. 5A). Furthermore, double mutant *ccp1Δgar2Δ* has a synergistic effect on the reduced variability of *cnt2::ade6* PEV (Fig. 5A and Fig. S3). Based on these findings, we postulated that Gar2 might locate outside nucleolus (such as centromeres) to modulate epigenetic stability, in addition to its

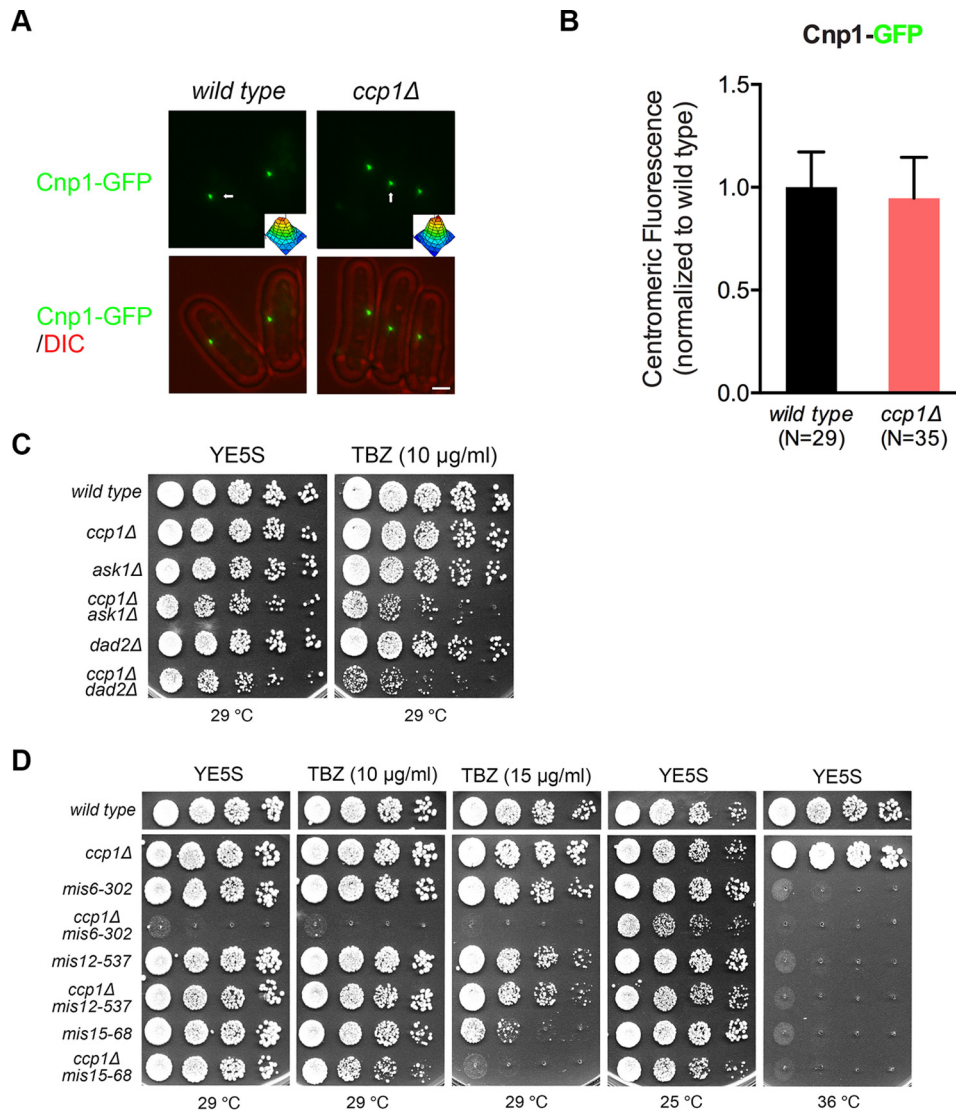


Figure 3. Deletion of *ccp1* has no effect on the total amount of Cnp1-GFP loading at centromeres. A, representative images of Cnp1-GFP in WT and *ccp1Δ* cells in the G₂ phase of the cell cycle. Insets at the bottom right, heat map quantitative display of the Cnp1-GFP dots indicated by white arrows. Merged images are shown in the bottom panel (GFP and DIC). Scale bar, 2 μm. B, the graph plots the relative mean fluorescent signal intensity of the Cnp1-GFP measured in *ccp1Δ* normalized to WT. N represents the total cells scored for the mean Cnp1-GFP intensity. Error bars, S.D. C, serial dilutions (5-fold) of the indicated strains were spotted on YE + 5S medium with no TBZ or with 10 μg/ml TBZ and grown at 29 °C. D, serial dilutions (5-fold) of the indicated strains were spotted on YE + 5S medium without TBZ or with 10 or 15 μg/ml TBZ and grown at 29 °C. Strains were also spotted on YE + 5S medium grown at 25, 29, and 36 °C.

expected functions in the nucleolus. To test this, we examined the subcellular localization of Gar2. Endogenous Gar2 was tagged with GFP at the C terminus and expressed under its native promoter. At all stages of the cell cycle, Gar2-GFP is predominately localized to the nucleolus as reported previously (43, 44, 46, 47), with an additional faint, diffused localization throughout the nucleus (Fig. 5B). No specific enrichment of Gar2-GFP at or near the spindle pole body marker Sad1-mCherry was detected (Fig. 5C). These data suggest that Gar2 does not specifically associate with centromeres.

We next examined possible genetic interdependency between Ccp1 and Gar2 for their specific subcellular localizations. Ccp1-GFP in *gar2Δ* or Gar2-GFP in *ccp1Δ* exhibited no difference compared with that in WT cells, indicating that they do not influence each other's localization (Fig. S4, A and B). Furthermore, we found that *gar2Δ* does not affect the total levels of Cnp1-GFP at centromeres either (Fig. 5D). Consistently, anti-

Cnp1 ChIP-Seq showed no significant difference in Cnp1 distribution pattern between *ccp1Δ*, *gar2Δ*, and WT (Fig. S5). On the other hand, *gar2Δ* is hypersensitive to TBZ (Fig. S4C), indicating that Gar2 may contribute to the proper functioning of centromeres/kinetochores.

Collectively, the investigations above demonstrate that Gar2 and Ccp1 function synergistically in modulating nucleosomal epigenetic stability at centromeres, although they are not stably associated with each other. Gar2 may perform its functions in a transient fashion or via an indirect mechanism.

***ccp1Δ* affects heterochromatin distribution both at pericentromeric and subtelomeric domains**

Because Ccp1 functions in modulating canonical H3-containing nucleosomal epigenetic stability indicated by using *cenH::ade6* PEV as the readout, we were interested in investigating whether Ccp1 plays a role in modulating heterochroma-

Nucleosomal epigenetic stability regulated by Ccp1

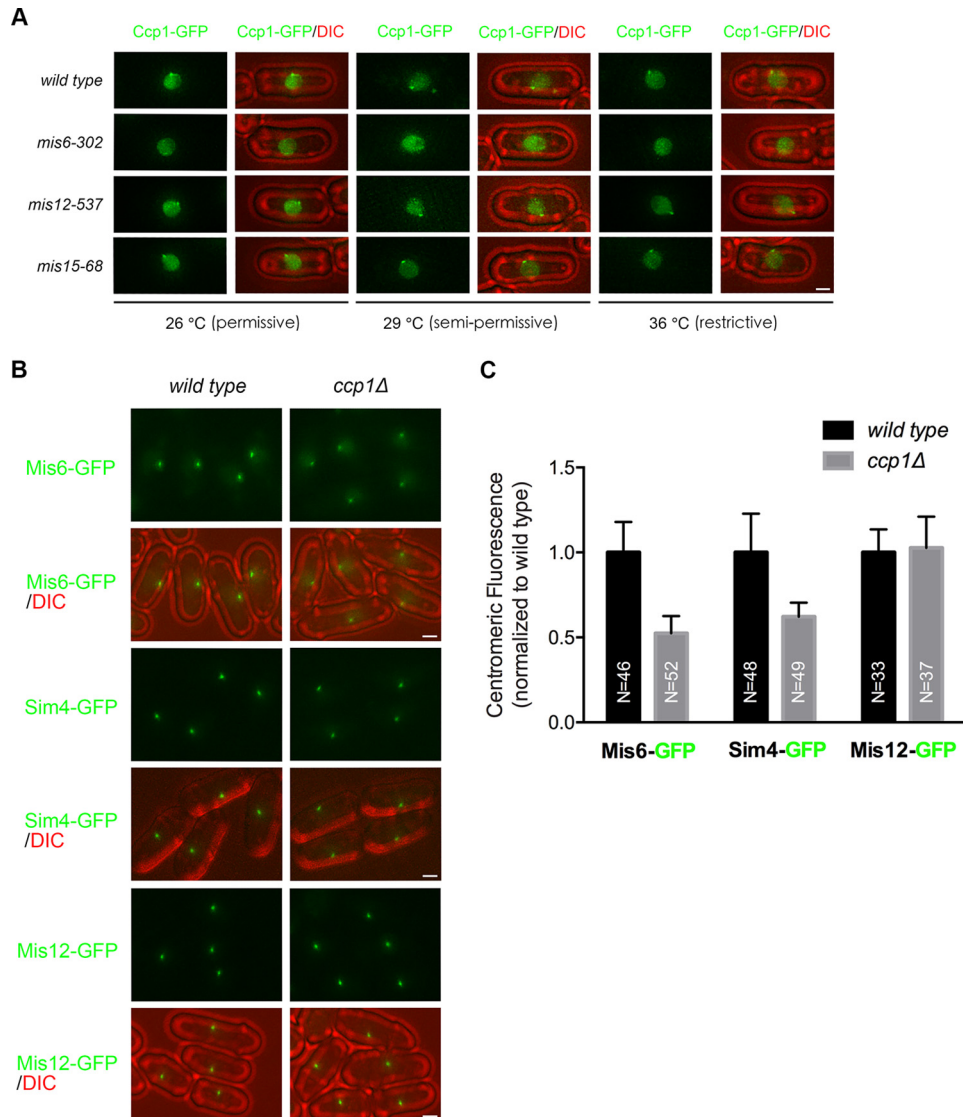


Figure 4. The interdependence between Ccp1 and Mis6 for centromere localization. *A*, representative images of Ccp1-GFP in WT, *mis6-302*, *mis12-537*, and *mis15-68* mutant cells cultured at 26, 29 (as labeled), or 26 °C shifted to 36 °C for 4 h (labeled as 36 °C). Ccp1-GFP (green) and Ccp1-GFP merged with DIC (green and red) are shown. Scale bar, 2 μm. *B*, representative images of Mis6-GFP, Sim4-GFP, and Mis12-GFP in WT and *ccp1Δ*. Scale bar, 2 μm. *C*, the graph plots the mean fluorescent signal intensity of the GFP dots of the indicated kinetochores proteins in *ccp1Δ* normalized to WT. Error bars, S.D. *N* represents the total cells scored for the mean GFP intensity. Scale bar, 2 μm.

tin distribution genome-wide. To this end, mononucleosomal IP-Seq (using H3K9me2-specific antibody) was performed in *ccp1Δ*, *gar2Δ*, *ccp1Δgar2Δ* compared with WT cells. (The strains used in all anti-Cnp1 and anti-H3K9me2 ChIP-Seq carry the *ade6* reporter inserted at *cnt2*. All of the high-throughput sequencing data have two biological repeats that are highly reproducible (e.g. Fig. S4D), one of which was randomly chosen for presentation in the main text.) Our data demonstrated that in *ccp1Δ* constitutive pericentromeric heterochromatin expands inward (but not at the other side toward euchromatin), causing a minor but significant heterochromatin presence in the central core region at *cnt2* (Fig. 6A). There was also slight spreading of pericentromeric heterochromatin into *cnt3* but not in *cnt1* (Fig. 6A). Importantly, *ccp1Δgar2Δ* exhibited pericentromeric heterochromatin spreading at *cnt2* and showed the synergistic effect on *cnt3* relative to their inner pericentromeric heterochromatin levels (Fig. 6A). This result indi-

cates that Ccp1 and Gar2 prevent the spreading of pericentromeric heterochromatin into centromeric core regions and thus are required for proper organization of centromere chromatin.

At the *Tel1* and *Tel2* subtelomeric domains, heterochromatin is dramatically (up to over 20 kb in length) diminished, and no alteration was detected at the subtelomeric heterochromatin of *Tel3* in *ccp1Δ*, whereas *gar2Δ* showed no difference compared with WT (Fig. 6B). Moreover, *ccp1Δgar2Δ* exhibited the same levels of subtelomeric heterochromatin shrinking as those of *ccp1Δ* (Fig. 6B), indicating that Ccp1, but not Gar2, has an important function in subtelomeric heterochromatin maintenance.

In addition to constitutive heterochromatin domains, small heterochromatin islands (namely facultative heterochromatin) also exist at multiple loci throughout the whole genome. These facultative heterochromatin islands are usually formed at meiosis-related loci and are thought to be involved in cellular dif-

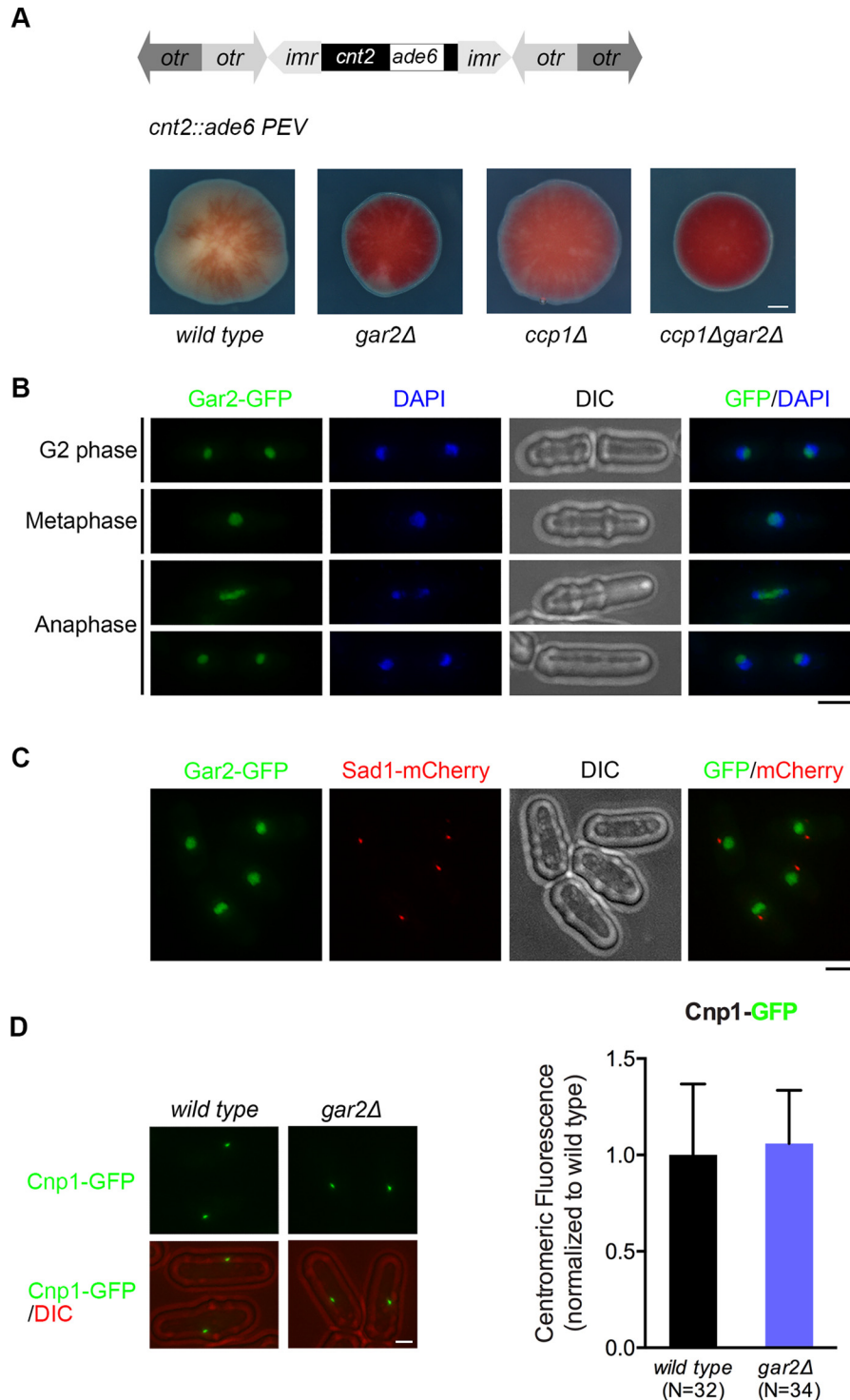


Figure 5. Gar2 genetically interacted with Ccp1 to participate in centromeric epigenetic regulation. *A*, schematics of the reporter gene *ade6* insertion sites at the genome. Representative colonies that are mostly red (hence derived from an *ade6*-silenced ancestor cell) are shown. Colony color sectoring morphology is compared among WT, *gar2Δ*, *ccp1Δ*, and *ccp1Δgar2Δ*. Scale bar, 50 μ m. *B*, subcellular localization of Gar2-GFP. Cells were fixed by methanol before 4',6-diamidino-2-phenylindole (DAPI) staining of DNA. Representative images of Gar2-GFP (green), DNA (blue), and merged images (right) in WT cells are shown. DIC images illustrate the cell outline. Scale bar, 8 μ m. *C*, co-localization of Gar2-GFP (green) and Sad1-mCherry (red). Cell outlines are shown in DIC images. Merged images (green and red) are displayed at the right. Scale bar, 5 μ m. *D*, representative images of Cnp1-GFP in WT and *gar2Δ* cells in G₂ phase of the cell cycle (left). Merged images are shown in the bottom panel (GFP and DIC). Scale bar, 2 μ m. The graph plots (right) the relative mean fluorescent signal intensity of the Cnp1-GFP measured in *gar2Δ* normalized to WT. *N* represents the total cells scored for the mean Cnp1-GFP intensity. Error bars, S.D.

ferentiation (48). The mechanisms for the precise assembly and inheritance of the small heterochromatin islands are still opaque. Several studies reported that Epe1 affects not only the silencing within the heterochromatin but also the establish-

ment of the boundary between heterochromatin islands and their neighboring euchromatin (48–50). Compared with the WT and *epe1Δ*, *ccp1Δ* showed a significant increase in H3K9me2 levels of small heterochromatin islands (such as

Nucleosomal epigenetic stability regulated by Ccp1

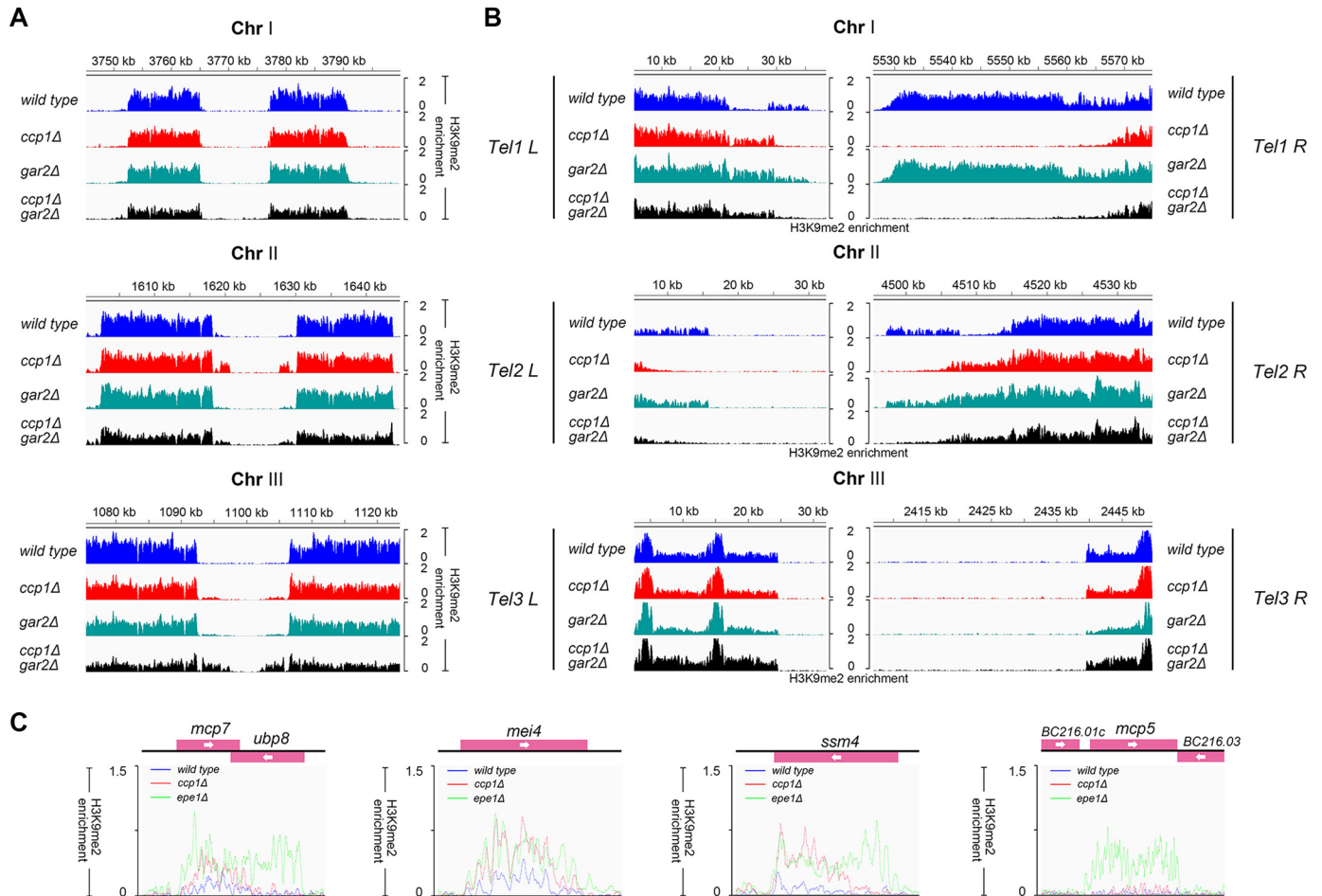


Figure 6. *ccp1Δ* affects heterochromatin distribution at the pericentromeric and subtelomeric regions. A, H3K9me2 mapping at centromeres by ChIP-Seq in WT, *ccp1Δ*, *gar2Δ*, and *ccp1Δgar2Δ*. All three *S. pombe* centromeres are shown. y axis, ChIP-Seq reads normalized for H3K9me2 enrichment; x axis, chromosomal position of the centromeres. B, H3K9me2 mapping at subtelomeres by ChIP-Seq in WT, *ccp1Δ*, *gar2Δ*, and *ccp1Δgar2Δ*. All three *S. pombe* subtelomere heterochromatin regions are shown. y axis, ChIP-Seq reads normalized for H3K9me2 enrichment. x axis, chromosomal position of the subtelomeres. C, H3K9me2 mapping at four facultative heterochromatin islands in WT, *ccp1Δ*, and *epe1Δ*. y axis, ChIP-Seq reads normalized for H3K9me2 enrichment. x axis, annotation of heterochromatin islands.

mei4 and *ssm4*) compared with WT but not as prominent as *epe1Δ* (Fig. 6C). Taken together, we conclude that Ccp1 is involved in the formation/maintenance of the WT level heterochromatin distribution at all subtelomeric regions.

Discussion

Epigenetic stability is regulated intricately

It is vital to preserve the fidelity of epigenetic inheritance through cell generations to maintain the cell identity and the organism homeostasis, as epigenetic aberrations likely contribute to a multitude of diseases (16, 51, 52). On the other hand, epigenetic inheritance fidelity should be amendable when needed. For example, epigenetic reprogramming is the essence of embryo development and cell differentiation. Thus, epigenetic fidelity should be modulated exquisitely. Using fission yeast CEN-PEV as the experimental tool, we are now able to quantify the epigenetic fidelity of one particular feature of the chromatin, the positioning of Cnp1 nucleosomes at reporter genes, and may start to elucidate the molecular mechanisms for modulating the epigenetic fidelity within the centromere core region. The PEV system that we have utilized serves as a proxy for Cnp1 occupancy at centromeres, with the potential caveat that it may

reflect the combined effects of Cnp1 occupancy and other unidentified (but epigenetically inheritable) mechanisms that modulate *ade6* reporter transcription.

We have found that deletions of histone chaperone or chromatin remodeling protein genes affect the switching frequency (i.e. the epigenetic stability) of CEN-PEV in a gene-specific manner (Table 1). In our previous paper (see Fig. 7B in Ref. 15), we erroneously reported that deletion of *pcf3*, a gene encoding one subunit of the CAF1 complex, enhances the rates of CEN-PEV epigenetic switching. Here, we found and confirmed repeatedly that *pcf3Δ* does not affect CEN-PEV, whereas *pcf1Δ* enhances the rates of epigenetic switching. Given the prominent role of CAF-1 in the process of replication-coupled nucleosome assembly, this indicates that the fidelity of chromatin duplication is a major determinant of epigenetic stability. This is in agreement with our recent finding that replication stresses elevate the variability of CEN-PEV (31). Also noticeable, among three subunits of the histone chaperone CAF-1, only *pcf1Δ* enhanced *cnt2::ade6* variability, whereas *pcf2Δ* or *pcf3Δ* exhibited WT level variability, suggesting that epigenetic stability modulation is a unique function of Pcf1 instead of the CAF-1 complex as an integral entity.

In contrast to *pcf1Δ*, deletion of a histone chaperone gene, *ccp1Δ*, or a nucleolus protein gene, *gar2Δ*, exhibited reduced epigenetic variability in CEN-PEV. Alternatively, another possible explanation is that the heterochromatin spreading into centromeric core regions in *ccp1Δ* should contribute to *ade6* silencing. Consistently, we detected low levels of heterochromatin on *ade6* reporter cassette by whole-genome heterochromatin mapping in *ccp1Δ*. It is plausible that the net increase of *ade6* silencing due to heterochromatin spreading would also affect the equilibrium of epigenetic stability by tipping the balance of the *ade6* ON/OFF switch toward the OFF direction. In other words, *ccp1Δ* should cause a reduction in OFF-to-ON switching frequency while causing an elevation in ON-to-OFF switching frequency. However, in contrast to this speculation, we observed that the frequencies of both OFF-to-ON and ON-to-OFF switching of *cnt2::ade6* were reduced in *ccp1Δ* compared with WT, whereas the reduction in ON-to-OFF switching is marginal; the result nonetheless indicates that changes in epigenetic variability in *ccp1Δ* might not be solely attributed to a net increase in silencing (Fig. 1C). Instead, we are in favor of a model in which *ccp1Δ* affects the CEN-PEV dynamics in two parallel mechanisms, a direct one that reduces the rates of *cnt2::ade6* ON/OFF switching in both directions and an indirect one that, via heterochromatin spreading, tips the ON/OFF balance toward the OFF direction.

It was proposed that replication-coupled nucleosome duplication could intrinsically be of low fidelity (53, 54) so that chromatin features carried by individual nucleosomes may not be inherited stably. Our finding demonstrates that the WT level of variability in CEN-PEV requires *ccp1* as well as *gar2*. Therefore, such variability does not reflect an intrinsically low fidelity in chromatin duplication. Instead, at least to some extent, epigenetic variation in CEN-PEV is a “deliberate” process, underscoring the intricacy of the mechanisms for modulating epigenetic stability. This further hints at the feasibility of fine-tuning epigenetic stability through genetic or pharmacologic intervention.

The diverse functional roles of Ccp1

In addition to its role in modulating centromeric epigenetic stability, Ccp1 performs additional functions at centromeres and also modulates epigenetic stability elsewhere in the genome.

Many studies have identified major players in CENP-A incorporation into centromeres; for example, the Mis16–Mis18 complex, Scm3 (a CENP-A–specific histone chaperone), and a NASP-(N1/N2)-related protein, Sim3, are critical for deposition and maintenance of CENP-A at centromeres (28, 55–63). A common effect of these proteins is that their inactivation/depletion leads to eventual loss of CENP-A/Cnp1 at centromeres. Different from this, deletion of *ccp1* or *gar2* does not cause a significant change in the total level of Cnp1 incorporation. A recent study has shown that Ccp1 functions in preventing or eliminating illegitimate Cnp1 incorporation into elsewhere other than centromeres in the context of high Cnp1 overexpression, as multiple nuclear Cnp1-GFP foci formed after *ccp1* was deleted (33). Dong *et al.* showed that 12% of cells exhibit Cnp1-GFP mislocalization when overexpressed at an

ectopic site, whereas only roughly 1% of cells with Cnp1-GFP expressed at the endogenous level exhibit Cnp1-GFP mislocalization (33).³ In our results, we did not detect the extra Cnp1-GFP dots elsewhere in *ccp1Δ* after microscopically examining >500 cells. This may be due to the difference under “Experimental procedures” as to whether the cells are harvested from solid medium (33)³ or from liquid medium.

The fact that incorporation of inner kinetochore proteins (Mis6 and sim4) is reduced in *ccp1Δ* suggests a functional role of Ccp1 in proper kinetochore assembly. On the other hand, partial inactivation of Mis6 (*mis6-302* temperature-sensitive mutation at 26 °C) (64) compromises the recruitment of Ccp1 at centromeres. These results indicate a mutual dependence of Ccp1 and inner kinetochore components for centromere binding and kinetochore incorporation. We note that Ccp1 is not a constitutive component of kinetochore, because it is dislocalized from the centromeres when cells enter mitosis (Fig. 2A). This is reminiscent of a couple of other centromere-associated proteins, such as Scm3 and Ams2 (59, 65). How Ccp1 is removed from centromeres specifically after the cell enters to mitosis remains elusive. In *ccp1Δ*, we have detected low but significant spreading of pericentromeric heterochromatin into the centromeric core regions (66). Hence, Ccp1 is also required to withhold the boundary between the centromeric core and the pericentromeric heterochromatin.

Overall, we propose a model in which Ccp1 enriched at the centromeres plays multiple functional roles locally; it modulates the nucleosomal epigenetic stability manifested as PEV, helps to maintain the boundary between the core regions and the pericentromeric heterochromatin domains, and contributes to kinetochore assembly. Our recent study has shown that the inner kinetochore is required for maintaining the boundary between the Cnp1-containing regions and pericentromeric heterochromatin,⁴ which might connect several functional roles of Ccp1.

Outside centromeres, Ccp1 also plays a functional role in modulating epigenetic stability and maintaining normal chromatin structures at multiple loci. In *ccp1Δ*, the subtelomeric heterochromatin domains of chromosomes I and II (*Tel1* and *Tel2*, left and right ends, respectively) have a drastic reduction in length at the centromeric-proximal end, at a range from 5 to 35 kb. In comparison, in other genetic lesions, such as *dbl5Δ* (Fig. S6) and *cdc22-3* (31), heterochromatin spreading occurred to various degrees in the same regions. Interestingly, the subtelomeric regions of chromosome III (*Tel3*) are highly stable, which indicates the locus-specific regulation of epigenetic stability by Ccp1. This may be due to the specialized nucleolar localization of *Tel3*.

In sum, we have demonstrated that epigenetic stability of centromeric chromatin is under intricate control. We have discovered new functions of Ccp1 in modulating epigenetic stability and maintaining proper organization of multiple chromatin domains to ensure the normal function of centromeres and heterochromatin. Determination of whether these roles are

³ F. Li, personal communication.

⁴ M. Lu and X. He, manuscript in preparation.

Nucleosomal epigenetic stability regulated by Ccp1

related to the chaperone function of Ccp1 requires further investigation.

Experimental procedures

Strains and media

Yeast genetic manipulations were conducted with standard procedures. The chromosomal integrated strains with epitopes (GFP, TAP, DsRed1, and Myc) were constructed as described (67). We also confirmed that the fusion constructs were fully functional by measuring cell growth or examining the CEN-PEV stability. Strains carrying different epitopes were obtained by genetic crossing and tetrad dissection. Cells were cultured at 29 °C unless other culture conditions were specified. For colony morphology observations, cells were cultured at 25 °C. The media used for culturing *S. pombe* were complete medium (YE+5S), YE+4S (low adenine), and ME sporulation medium. For marker selection or drug sensitivity test, the indicated drugs were added into the medium. *S. pombe* strains and primers used in this study are listed in Table S2 and Table S3, respectively.

Pedigree analysis

Pedigree analysis was performed as described (15). Strains were cultured in YE+4S (low adenine) liquid for 2–4 generations, and then cells were spread in a line near the top of a YE+4S plate. The ancestral cell (generation I) and its descendants (generations II–IV) were moved to the designated positions by micromanipulation using a glass needle. The pedigree information was retained by relative positioning of the descendant cells. The plates were incubated at 25 °C for 5 days to form single colonies. Colony morphology was recorded using a stereomicroscope with a CCD camera. The rates of red-to-white and white-to-red switching between mutant and WT strains were scored by the numbers of switching events in 600–1,000 cell divisions.

Microscopy

Cells were cultured at 29 °C in complete medium (YE+5S). For temperature-sensitive strains, cells were initially cultured at 26 °C in complete medium and then were shifted to 36 °C for appropriate generations. Images were taken with a Delta Vision Elite microscope (Applied Precision) with a $\times 60$, 1.42 numerical aperture objective oil lens. Multiple optical sections were collected for the measurement of fluorescence intensities, and the vertical distance between sections was 0.25–0.3 μm . Deconvolution, image projections (maximum intensity), and quantification of fluorescence signals were performed using an imaging work station (SoftWoRx, Applied Precision).

Mass spectrometry

Standard TAP purification procedures were used as described previously (68–70). After affinity purification, the eluted samples were separated by 12.5% SDS-PAGE. The gel containing proteins was cut, and MS analysis was performed at the Beijing Proteome Research Center (Beijing, China).

ChIP and ChIP-Seq

The standard procedures of ChIP were used as described (71, 72). For Myc-ChIP, cells were cultured at 29 °C in complete

medium (YE+5S) and fixed with 1% paraformaldehyde solution for 60 min. The fixation reaction was quenched with 125 mM glycine. Cell pellets were lysed mechanically with glass beads using a bead beater. Chromatin was sheared to 200–400-bp fragments by sonication following the specifications recommended by the sonicator manufacturer (Diagenode Bioruptor Pico). Anti-Myc (ab9132, Abcam) was used in immunoprecipitation. For H3K9me2-ChIP and Cnp1-ChIP, cells were cultured at 29 °C in complete medium and harvested. Cell pellets were suspended in 1 M sorbitol, 50 mM Tris (pH 7.5) with freshly added 10 mM DTT. Zymolase (final concentration 0.25 mg/ml) was added to digest the yeast cell walls. After zymolyase treatment, cells were lysed and treated with 30 units/ μl micrococcal nuclease (Thermo Fisher Scientific) to digest chromatin into mononucleosomes. Anti-H3K9me2 (ab1220, Abcam) and anti-Cnp1 (provided by the Allshire laboratory) were used in immunoprecipitation.

The sequencer (Ion PGM™ system, Life Technologies, Inc.) was used for next-generation sequencing according to the manufacturer's protocols. Libraries of DNA were prepared using a commercial high-throughput library preparation kit (KAPA).

High-throughput sequencing data analysis

ChIP-Seq raw data were aligned to the assembly genome *S. pombe* ASM294v.2.22 with BWA. Duplication reads were removed. Mapped reads were normalized between different data sets. Peak calling was performed for visualization in the Integrative Genome Viewer (IGV) (73). The algorithm used was Model-based Analysis of ChIP-Seq (MACS) (74). All ChIP-Seq data and the details of the data analysis procedures have been submitted to the NCBI Gene Expression Omnibus (GEO) under accession number GSE95047.

Author contributions—M. L. and X. H. conceptualization; M. L. data curation; M. L. software; M. L. investigation; M. L. writing-original draft; M. L. and X. H. project administration; M. L. and X. H. writing-review and editing; X. H. supervision; X. H. funding acquisition.

Acknowledgments—We are grateful to X. Shirley Liu and members of the Liu laboratory for bioinformatics training.

References

1. Luger, K., Mäder, A. W., Richmond, R. K., Sargent, D. F., and Richmond, T. J. (1997) Crystal structure of the nucleosome core particle at 2.8 Å resolution. *Nature* **389**, 251–260 [CrossRef Medline](#)
2. De Koning, L., Corpet, A., Haber, J. E., and Almouzni, G. (2007) Histone chaperones: an escort network regulating histone traffic. *Nat. Struct. Mol. Biol.* **14**, 997–1007 [CrossRef Medline](#)
3. Clément, C., and Almouzni, G. (2015) MCM2 binding to histones H3-H4 and ASF1 supports a tetramer-to-dimer model for histone inheritance at the replication fork. *Nat. Struct. Mol. Biol.* **22**, 587–589 [CrossRef Medline](#)
4. Ransom, M., Dennehey, B. K., and Tyler, J. K. (2010) Chaperoning histones during DNA replication and repair. *Cell* **140**, 183–195 [CrossRef Medline](#)
5. Burgess, R. J., and Zhang, Z. (2013) Histone chaperones in nucleosome assembly and human disease. *Nat. Struct. Mol. Biol.* **20**, 14–22 [CrossRef Medline](#)
6. Gurard-Levin, Z. A., Quivy, J. P., and Almouzni, G. (2014) Histone chaperones: assisting histone traffic and nucleosome dynamics. *Annu. Rev. Biochem.* **83**, 487–517 [CrossRef Medline](#)

7. Hayashi, A., Asakawa, H., Haraguchi, T., and Hiraoka, Y. (2006) Reconstruction of the kinetochore during meiosis in fission yeast *Schizosaccharomyces pombe*. *Mol. Biol. Cell* **17**, 5173–5184 [CrossRef Medline](#)
8. Cleveland, D. W., Mao, Y., and Sullivan, K. F. (2003) Centromeres and kinetochores: from epigenetics to mitotic checkpoint signaling. *Cell* **112**, 407–421 [CrossRef Medline](#)
9. Liu, X., McLeod, I., Anderson, S., Yates, J. R., 3rd, and He, X. (2005) Molecular analysis of kinetochore architecture in fission yeast. *EMBO J.* **24**, 2919 [CrossRef Medline](#)
10. Henikoff, S., and Henikoff, J. G. (2012) “Point” centromeres of *Saccharomyces* harbor single centromere-specific nucleosomes. *Genetics* **190**, 1575–1577 [CrossRef Medline](#)
11. Cheeseman, I. M., Drubin, D. G., and Barnes, G. (2002) Simple centromere, complex kinetochore: linking spindle microtubules and centromeric DNA in budding yeast. *J. Cell Biol.* **157**, 199–203 [CrossRef Medline](#)
12. Furuyama, S., and Biggins, S. (2007) Centromere identity is specified by a single centromeric nucleosome in budding yeast. *Proc. Natl. Acad. Sci. U.S.A.* **104**, 14706–14711 [CrossRef Medline](#)
13. Blower, M. D., Sullivan, B. A., and Karpen, G. H. (2002) Conserved organization of centromeric chromatin in flies and humans. *Dev. Cell* **2**, 319–330 [CrossRef Medline](#)
14. Castillo, A. G., Mellone, B. G., Partridge, J. F., Richardson, W., Hamilton, G. L., Allshire, R. C., and Pidoux, A. L. (2007) Plasticity of fission yeast CENP-A chromatin driven by relative levels of histone H3 and H4. *PLoS Genet.* **3**, e121 [CrossRef Medline](#)
15. Yao, J., Liu, X., Sakuno, T., Li, W., Xi, Y., Aravamudan, P., Joglekar, A., Li, W., Watanabe, Y., and He, X. (2013) Plasticity and epigenetic inheritance of centromere-specific histone H3 (CENP-A)-containing nucleosome positioning in the fission yeast. *J. Biol. Chem.* **288**, 19184–19196 [CrossRef Medline](#)
16. Alabert, C., and Groth, A. (2012) Chromatin replication and epigenome maintenance. *Nat. Rev. Mol. Cell Biol.* **13**, 153–167 [CrossRef Medline](#)
17. Verdel, A., Jia, S., Gerber, S., Sugiyama, T., Gygi, S., Grewal, S. I., and Moazed, D. (2004) RNAi-mediated targeting of heterochromatin by the RITS complex. *Science* **303**, 672–676 [CrossRef Medline](#)
18. Maison, C., and Almouzni, G. (2004) HP1 and the dynamics of heterochromatin maintenance. *Nat. Rev. Mol. Cell Biol.* **5**, 296–304 [CrossRef Medline](#)
19. Pal-Bhadra, M., Leibovitch, B. A., Gandhi, S. G., Chikka, M. R., Rau, M., Bhadra, U., Birchler, J. A., and Elgin, S. C. (2004) Heterochromatic silencing and HP1 localization in *Drosophila* are dependent on the RNAi machinery. *Science* **303**, 669–672 [CrossRef Medline](#)
20. Elgin, S. C. R., and Grewal, S. I. S. (2003) Heterochromatin: silence is golden. *Curr. Biol.* **13**, R895–R898 [CrossRef Medline](#)
21. Grewal, S. I., and Jia, S. (2007) Heterochromatin revisited. *Nat. Rev. Genet.* **8**, 35–46 [CrossRef Medline](#)
22. Shankaranarayana, G. D., Motamedi, M. R., Moazed, D., and Grewal, S. I. S. (2003) Sir2 regulates histone H3 lysine 9 methylation and heterochromatin assembly in fission yeast. *Curr. Biol.* **13**, 1240–1246 [CrossRef Medline](#)
23. Scott, K. C., Merrett, S. L., and Willard, H. F. (2006) A heterochromatin barrier partitions the fission yeast centromere into discrete chromatin domains. *Curr. Biol.* **16**, 119–129 [CrossRef Medline](#)
24. Liu, T. Y., Dodson, A. E., Terhorst, J., Song, Y. S., and Rine, J. (2016) Riches of phenotype computationally extracted from microbial colonies. *Proc. Natl. Acad. Sci. U.S.A.* **113**, E2822–E2831 [CrossRef Medline](#)
25. Muller, H. J. (1929) Types of visible variations induced by X-rays in *Drosophila*. *J. Genet.* **22**, 299–334
26. Allshire, R. C., Javerzat, J.-P., Redhead, N. J., and Cranston, G. (1994) Position effect variegation at fission yeast centromeres. *Cell* **76**, 157–169 [CrossRef Medline](#)
27. Pidoux, A. L. R., Richardson, W., and Allshire, R. C. (2003) Sim4: a novel fission yeast kinetochore protein required for centromeric silencing and chromosome segregation. *J. Cell Biol.* **161**, 295–307 [CrossRef Medline](#)
28. Dunleavy, E. M., Pidoux, A. L., Monet, M., Bonilla, C., Richardson, W., Hamilton, G. L., Ekwall, K., McLaughlin, P. J., and Allshire, R. C. (2007) A NASP (N1/N2)-related protein, Sim3, binds CENP-A and is required for its deposition at fission yeast centromeres. *Mol. Cell* **28**, 1029–1044 [CrossRef Medline](#)
29. Allshire, R. C., and Ekwall, K. (2015) Epigenetic regulation of chromatin states in *Schizosaccharomyces pombe*. *Cold Spring Harb. Perspect. Biol.* **7**, a018770 [CrossRef Medline](#)
30. Kim, D. U., Hayles, J., Kim, D., Wood, V., Park, H. O., Won, M., Yoo, H. S., Duhig, T., Nam, M., Palmer, G., Han, S., Jeffery, L., Baek, S. T., Lee, H., Shim, Y. S., et al. (2010) Analysis of a genome-wide set of gene deletions in the fission yeast *Schizosaccharomyces pombe*. *Nat. Biotechnol.* **28**, 617–623 [CrossRef Medline](#)
31. Li, W., Yi, J., Agbu, P., Zhou, Z., Kelley, R. L., Kallgren, S., Jia, S., and He, X. (2017) Replication stress affects the fidelity of nucleosome-mediated epigenetic inheritance. *PLoS Genet.* **13**, e1006900 [CrossRef Medline](#)
32. Hall, I. M., Shankaranarayana, G. D., Noma, K., Ayoub, N., Cohen, A., and Grewal, S. I. S. (2002) Establishment and maintenance of a heterochromatin domain. *Science* **297**, 2232–2237 [CrossRef Medline](#)
33. Dong, Q., Yin, F. X., Gao, F., Shen, Y., Zhang, F., Li, Y., He, H., Gonzalez, M., Yang, J., Zhang, S., Su, M., Chen, Y.-H., and Li, F. (2016) Ccp1 homodimer mediates chromatin integrity by antagonizing CENP-A loading. *Mol. Cell* **64**, 79–91 [CrossRef Medline](#)
34. Han, J., Zhou, H., Li, Z., Xu, R. M., and Zhang, Z. (2007) The Rtt109-Vps75 histone acetyltransferase complex acetylates non-nucleosomal histone H3. *J. Biol. Chem.* **282**, 14158–14164 [CrossRef Medline](#)
35. Selth, L., and Svejstrup, J. Q. (2007) Vps75, a new yeast member of the NAP histone chaperone family. *J. Biol. Chem.* **282**, 12358–12362 [CrossRef Medline](#)
36. Selth, L. A., Lorch, Y., Ocampo-Hafalla, M. T., Mitter, R., Shales, M., Krogan, N. J., Kornberg, R. D., and Svejstrup, J. Q. (2009) An rtt109-independent role for vps75 in transcription-associated nucleosome dynamics. *Mol. Cell Biol.* **29**, 4220–4234 [CrossRef Medline](#)
37. Tang, Y., Meeth, K., Jiang, E., Luo, C., and Marmorstein, R. (2008) Structure of Vps75 and implications for histone chaperone function. *Proc. Natl. Acad. Sci. U.S.A.* **105**, 12206–12211 [CrossRef Medline](#)
38. Xue, Y. M., Kowalska, A. K., Grabowska, K., Przybyt, K., Cichewicz, M. A., Del Rosario, B. C., and Pemberton, L. F. (2013) Histone chaperones Nap1 and Vps75 regulate histone acetylation during transcription elongation. *Mol. Cell Biol.* **33**, 1645–1656 [CrossRef Medline](#)
39. Keck, K. M., and Pemberton, L. F. (2011) Interaction with the histone chaperone Vps75 promotes nuclear localization and HAT activity of Rtt109 in vivo. *Traffic* **12**, 826–839 [CrossRef Medline](#)
40. Roguev, A., Bandyopadhyay, S., Zofall, M., Zhang, K., Fischer, T., Collins, S. R., Qu, H., Shales, M., Park, H. O., Hayles, J., Hoe, K. L., Kim, D. U., Ideker, T., Grewal, S. I., Weissman, J. S., and Krogan, N. J. (2008) Conservation and rewiring of functional modules revealed by an epistasis map in fission yeast. *Science* **322**, 405–410 [CrossRef Medline](#)
41. Buttrick, G. J., and Millar, J. B. (2011) Ringing the changes: emerging roles for DASH at the kinetochore-microtubule interface. *Chromosome Res.* **19**, 393–407 [CrossRef Medline](#)
42. Gao, Q., Courtheoux, T., Gachet, Y., Tournier, S., and He, X. (2010) A non-ring-like form of the Dam1 complex modulates microtubule dynamics in fission yeast. *Proc. Natl. Acad. Sci. U.S.A.* **107**, 13330–13335 [CrossRef Medline](#)
43. Nakazawa, N., Nakamura, T., Kokubu, A., Ebe, M., Nagao, K., and Yanagida, M. (2008) Dissection of the essential steps for condensin accumulation at kinetochores and rDNAs during fission yeast mitosis. *J. Cell Biol.* **180**, 1115–1131 [CrossRef Medline](#)
44. Gulli, M. P., Girard, J. P., Zabetakis, D., Lapeyre, B., Melese, T., and Caizergues-Ferrer, M. (1995) gar2 is a nucleolar protein from *Schizosaccharomyces pombe* required for 18S rRNA and 40S ribosomal subunit accumulation. *Nucleic Acids Res.* **23**, 1912–1918 [CrossRef Medline](#)
45. Sicard, H., Faubladiere, M., Noaillac-Depeyre, J., Léger-Silvestre, I., Gas, N., and Caizergues-Ferrer, M. (1998) The role of the *Schizosaccharomyces pombe* gar2 protein in nucleolar structure and function depends on the concerted action of its highly charged N terminus and its RNA-binding domains. *Mol. Biol. Cell* **9**, 2011–2023 [CrossRef Medline](#)
46. Jin, Q.-W., Ray, S., Choi, S. H., and McCollum, D. (2007) The nucleolar Net1/Cfi1-related protein Dnt1 antagonizes the septation initiation network in fission yeast. *Mol. Biol. Cell* **18**, 2924–2934 [CrossRef Medline](#)

Nucleosomal epigenetic stability regulated by Ccp1

47. Sugiyama, T., Wanatabe, N., Kitahata, E., Tani, T., and Sugioka-Sugiyama, R. (2013) Red5 and three nuclear pore components are essential for efficient suppression of specific mRNAs during vegetative growth of fission yeast. *Nucleic Acids Res.* **41**, 6674–6686 [CrossRef Medline](#)
48. Zofall, M., Yamanaka, S., Reyes-Turcu, F. E., Zhang, K., Rubin, C., and Grewal, S. I. (2012) RNA elimination machinery targeting meiotic mRNAs promotes facultative heterochromatin formation. *Science* **335**, 96–100 [CrossRef Medline](#)
49. Ayoub, N., Noma, K., Isaac, S., Kahan, T., Grewal, S. I. S., and Cohen, A. (2003) A novel jmjC domain protein modulates heterochromatinization in fission yeast. *Mol. Cell. Biol.* **23**, 4356–4370 [CrossRef Medline](#)
50. Trewick, S. C., Minc, E., Antonelli, R., Urano, T., and Allshire, R. C. (2007) The JmjC domain protein Epe1 prevents unregulated assembly and disassembly of heterochromatin. *EMBO J.* **26**, 4670–4682 [CrossRef Medline](#)
51. Jasencakova, Z., Scharf, A. N., Ask, K., Corpet, A., Imhof, A., Almouzni, G., and Groth, A. (2010) Replication stress interferes with histone recycling and predeposition marking of new histones. *Mol. Cell* **37**, 736–743 [CrossRef Medline](#)
52. Hatziaepostolou, M., and Iliopoulos, D. (2011) Epigenetic aberrations during oncogenesis. *Cell. Mol. Life Sci.* **68**, 1681–1702 [CrossRef Medline](#)
53. Zhu, B., and Reinberg, D. (2011) Epigenetic inheritance: uncontested? *Cell Res.* **21**, 435–441 [CrossRef Medline](#)
54. Radman-Livaja, M., Verzijlbergen, K. F., Weiner, A., van Welsem, T., Friedman, N., Rando, O. J., and van Leeuwen, F. (2011) Patterns and mechanisms of ancestral histone protein inheritance in budding yeast. *PLoS Biol.* **9**, e1001075 [CrossRef Medline](#)
55. Fujita, Y., Hayashi, T., Kiyomitsu, T., Toyoda, Y., Kokubu, A., Obuse, C., and Yanagida, M. (2007) Priming of centromere for CENP-A recruitment by human hMis18 α , hMis18 β , and M18BP1. *Dev. Cell* **12**, 17–30 [CrossRef Medline](#)
56. Camahort, R., Li, B., Florens, L., Swanson, S. K., Washburn, M. P., and Gerton, J. L. (2007) Scm3 is essential to recruit the histone h3 variant cse4 to centromeres and to maintain a functional kinetochore. *Mol. Cell* **26**, 853–865 [CrossRef Medline](#)
57. Mizuguchi, G., Xiao, H., Wisniewski, J., Smith, M. M., and Wu, C. (2007) Nonhistone Scm3 and histones CenH3-H4 assemble the core of centromere-specific nucleosomes. *Cell* **129**, 1153–1164 [CrossRef Medline](#)
58. Dunleavy, E. M., Roche, D., Tagami, H., Lacoste, N., Ray-Gallet, D., Nakamura, Y., Daigo, Y., Nakatani, Y., and Almouzni-Pettinotti, G. (2009) HJURP is a cell-cycle-dependent maintenance and deposition factor of CENP-A at centromeres. *Cell* **137**, 485–497 [CrossRef Medline](#)
59. Pidoux, A. L., Choi, E. S., Abbott, J. K., Liu, X., Kagansky, A., Castillo, A. G., Hamilton, G. L., Richardson, W., Rappsilber, J., He, X., and Allshire, R. C. (2009) Fission yeast Scm3: a CENP-A receptor required for integrity of subkinetochore chromatin. *Mol. Cell* **33**, 299–311 [CrossRef Medline](#)
60. Williams, J. S., Hayashi, T., Yanagida, M., and Russell, P. (2009) Fission yeast Scm3 mediates stable assembly of Cnp1/CENP-A into centromeric chromatin. *Mol. Cell* **33**, 287–298 [CrossRef Medline](#)
61. Black, B. E., Jansen, L. E., Maddox, P. S., Foltz, D. R., Desai, A. B., Shah, J. V., and Cleveland, D. W. (2007) Centromere identity maintained by nucleosomes assembled with histone H3 containing the CENP-A targeting domain. *Mol. Cell* **25**, 309–322 [CrossRef Medline](#)
62. Bassett, E. A., DeNizio, J., Barnhart-Dailey, M. C., Panchenko, T., Sekulic, N., Rogers, D. J., Foltz, D. R., and Black, B. E. (2012) HJURP uses distinct CENP-A surfaces to recognize and to stabilize CENP-A/histone H4 for centromere assembly. *Dev. Cell* **22**, 749–762 [CrossRef Medline](#)
63. Kim, S., and Yu, H. (2015) Multiple assembly mechanisms anchor the KMN spindle checkpoint platform at human mitotic kinetochores. *J. Cell Biol.* **208**, 181–196 [CrossRef Medline](#)
64. Saitoh, S., Takahashi, K., and Yanagida, M. (1997) Mis6, a fission yeast inner centromere protein, acts during G₁/S and forms specialized chromatin required for equal segregation. *Cell* **90**, 131–143 [CrossRef Medline](#)
65. Chen, E. S., Saitoh, S., Yanagida, M., and Takahashi, K. (2003) A cell cycle-regulated GATA factor promotes centromeric localization of CENP-A in fission yeast. *Mol. Cell* **11**, 175–187 [CrossRef Medline](#)
66. Sadeghi, L., Siggins, L., Svensson, J. P., and Ekwall, K. (2014) Centromeric histone H2B monoubiquitination promotes noncoding transcription and chromatin integrity. *Nat. Struct. Mol. Biol.* **21**, 236–243 [CrossRef Medline](#)
67. Knop, M., Siegers, K., Pereira, G., Zachariae, W., Winsor, B., Nasmyth, K., and Schiebel, E. (1999) Epitope tagging of yeast genes using a PCR-based strategy: more tags and improved practical routines. *Yeast* **15**, 963–972 [CrossRef Medline](#)
68. Puig, O., Caspary, F., Rigaut, G., Rutz, B., Bouveret, E., Bragado-Nilsson, E., Wilm, M., and Séraphin, B. (2001) The tandem affinity purification (TAP) method: a general procedure of protein complex purification. *Methods* **24**, 218–229 [CrossRef Medline](#)
69. Link, A. J., Weaver, C., and Farley, A. (2011) IgG affinity capture of TAP-tagged protein complexes from cell extracts: affinity purification step 1. *Cold Spring Harb. Protoc.* **2011**, pdb.prot5606 [CrossRef Medline](#)
70. Link, A. J., Weaver, C., and Farley, A. (2011) Affinity capture of TAP-tagged protein complexes: affinity purification step 2. *Cold Spring Harb. Protoc.* **2011**, pdb.prot5607 [CrossRef Medline](#)
71. Volpe, T. A., and DeMaio, J. (2011) Chromatin immunoprecipitation in fission yeast. in *Argonaute Proteins: Methods and Protocols* (Hobman, T. C., and Duchaine, T. F., eds) pp. 15–28, Humana Press, Totowa, NJ
72. Infante, J. J., Law, G. L., and Young, E. T. (2012) Analysis of nucleosome positioning using a nucleosome-scanning assay. *Methods Mol. Biol.* **833**, 63–87 [CrossRef Medline](#)
73. Thorvaldsdóttir, H., Robinson, J. T., and Mesirov, J. P. (2013) Integrative Genomics Viewer (IGV): high-performance genomics data visualization and exploration. *Brief. Bioinform.* **14**, 178–192 [CrossRef Medline](#)
74. Zhang, Y., Liu, T., Meyer, C. A., Eickhout, J., Johnson, D. S., Bernstein, B. E., Nusbaum, C., Myers, R. M., Brown, M., Li, W., and Liu, X. S. (2008) Model-based analysis of ChIP-Seq (MACS). *Genome Biol.* **9**, R137 [CrossRef Medline](#)